

International Conference on Space Optics—ICSO 2012

Ajaccio, Corse

9–12 October 2012

Edited by Bruno Cugny, Errico Armandillo, and Nikos Karafolas



Investigation on high efficiency volume Bragg gratings performances for spectrometry in space environment

Jérôme Loicq

Y. Stockman

Marc Georges

Luis Miguel Gaspar Venancio



Investigation on High Efficiency Volume Bragg gratings performances for spectrometry in space environment

Jérôme Loicq, Y. Stockman, Marc Georges
Centre spatial de Liège-University of Liège
Liege, Belgium
Contact author: J.Loicq@ulg.ac.be

Luis Miguel Gaspar Venancio
European Space Agency,
ESA – ESTEC
Noordwijk ZH, The Netherlands

Abstract— The special properties of Volume Bragg Gratings (VBGs) make them good candidates for spectrometry applications where high spectral resolution, low level of straylight and low polarisation sensitivity are required. Therefore it is of interest to assess the maturity and suitability of VBGs as enabling technology for future ESA missions with demanding requirements for spectrometry. The VBGs suitability for space application is being investigated in the frame of a project led by CSL and funded by the European Space Agency. The goal of this work is twofold: first the theoretical advantages and drawbacks of VBGs with respect to other technologies with identical functionalities are assessed, and second the performances of VBG samples in a representative space environment are experimentally evaluated. The performances of samples of two VBGs technologies, the Photo-Thermo-Refractive (PTR) glass and the DiChromated Gelatine (DCG), are assessed and compared in the H α , O₂-B and NIR bands. The tests are performed under vacuum condition combined with temperature cycling in the range of 200 K to 300K. A dedicated test bench experiment is designed to evaluate the impact of temperature on the spectral efficiency and to determine the optical wavefront error of the diffracted beam. Furthermore the diffraction efficiency degradation under gamma irradiation is assessed. Finally the straylight, the diffraction efficiency under conical incidence and the polarisation sensitivity is evaluated.

Index Terms— Volume Bragg Grating, Space environment, gamma radiation, thermal vacuum, diffraction efficiency, WFE

I. INTRODUCTION

Holography is today a well-established technique, which has found many applications. An example of an innovative application is the Volume Phase Holographic (VPH) grating or Volume Bragg grating (VBG). VPH gratings are produced by illuminating a photo-sensitive substrate with overlapping coherent light beams [1-3]. The resulting interference pattern is then permanently recorded in the volume of the substrate as a periodic variation of the refractive index of the substrate material. Once recorded the VPHs spatially disperse the spectrum of an incident light beam, like other dispersive

elements as prisms and conventional gratings. In comparison to prisms and ruled Surface Relief (SR) gratings the VPHs have interesting advantages. The main advantages are higher peak diffraction efficiency, lower polarisation effects, lower level of scattered light and higher spectral and spatial selectivity. This work takes place in the frame of an ESA study in the case of Earth observation missions.

The objectives of the research are to evaluate the possibilities to use VBG grating in the frame of ESA missions for space applications [4-7]. Such gratings could be foreseen for hyper-spectral imaging. As it will be demonstrated, the special properties of VBGs make them interesting for spectrometry applications where high spectral resolution, low level of straylight and low polarisation sensitivity are required. Because of space environment VBG have to keep their properties during flight to ensure the mission viability [8-9]. In particular they have to resist to thermal vacuum environment, radiation (electron, proton, gamma, heavy ions,...), atomic oxygen, vibration, etc. In this paper we focused the analysis on the optical properties (diffraction efficiency, WaveFront Error) under thermal cycles and gamma radiation.

The ESA requirements were essentially focused on the Wavefront quality, polarization sensitivity (defined by $|\eta_{\max}^{TE} - \eta_{\max}^{TM}| / |\eta_{\max}^{TE} + \eta_{\max}^{TM}|$ with a target lower than 5.10^{-3}) and diffraction efficiency which has to be higher than 90% on the specified spectral band. Two VBG candidate technologies were analysed and compared:

- DCG grating: VBGs made of a thin film (tens of microns thick) of photosensitive dichromated gelatine (DCG) sandwiched between two pieces of glass. This type of VBG is widely used in ground based astronomy applications. [10-11]
- Photo-Thermo-Refractive (PTR) glass. They allow the manufacturing of thicker (several millimeters thick)

VBGs, leading to a narrower spectrum of the diffracted beam. [12-15]

Three bands have been selected: H α (PTR) (646-666 nm), O2B (DCG) (677-697 nm) and NIR (DCG)(750-775). The performances of those grating were experimentally assessed in thermo-vacuum condition and under gamma irradiation.

II. METHODOLOGY ANALYSIS AND EXPERIMENTAL BENCHES

Diffraction efficiency and WFE of the VBGs are the main properties investigated during the environmental experiments. However scattering properties and out-of-band characteristics are also assessed as characterization tests. General aspect and defaults are also monitored by visual inspection after each test sequences. The experimental plan presented on Figure 1 has been followed to perform the characterization and environmental test. Characterization tests have been performed after each environmental test for comparison.

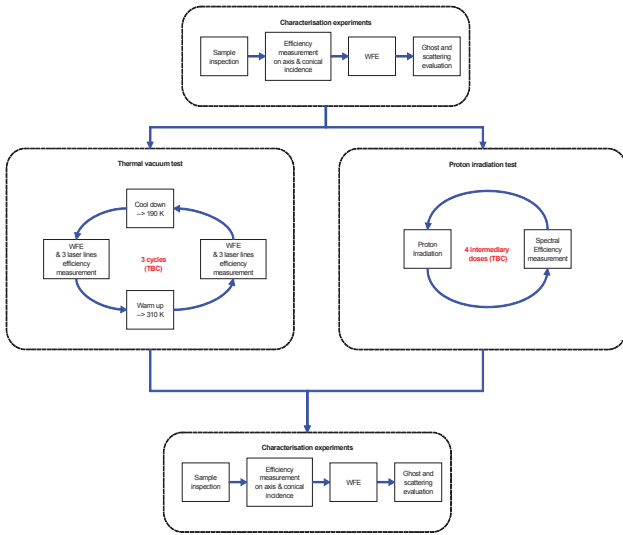


Figure 1: Experimental validation plan

A. Efficiency measurements:

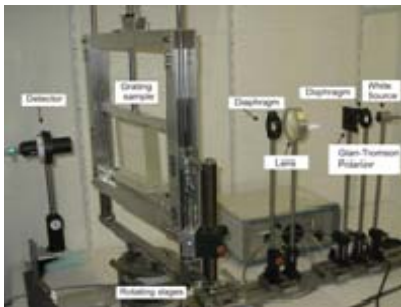


Figure 2: The spectral characterization bench.

The spectral characterization bench consists of a fibered white collimated light source and polarized (TE or TM). Transmitted or diffracted light is collected with a collimator

assembly and injected into a fiber which directs the light to a spectrometric detector. The grating is mounted on a rotation stage, while the detector collimator assembly is mounted on a goniometer whose rotation axis is similar to the grating rotation stage.

B. WFE measurements:

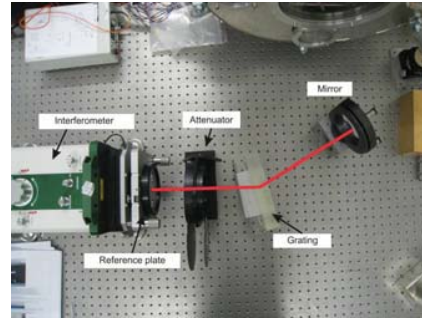


Figure 3: WFE measurements bench

Diffracted WFE is characterized by the experiment exposed on Figure 3. This configuration is then transposed in the vacuum chamber. The beam of interest passes twice by the grating thanks to the mirror. A reference WFE measurement on the cavity mirror is performed in a preliminary step.

C. Scattering evaluation bench:

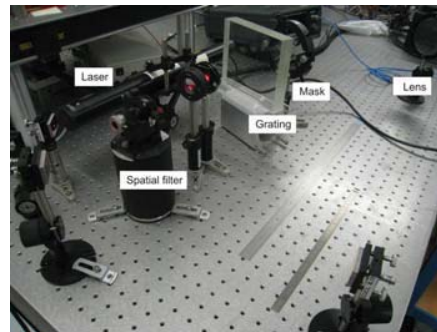


Figure 4: Scattering evaluation bench

The measurement consist in the comparison of the global flux transmitted through the grating including direct and diffused beams in a specific order and the diffused light without principal beam. The experimental setup proposed is a 2-f setup (see Figure 4). A lens is placed at a distance which is two times the focal length. In this condition, the image of the grating exit spot is imaged at a distance 2f of the lens with a linear magnification equal to unity. A detector is placed at this position. All the diffused rays generated in the incidence cone retrieved by the lens are directed to this specific point. The principal beam is blocked with a circular mask of metal coated on transparent glass. Comparisons of the flux with and without mask give a figure of diffusing properties.

D. Thermal vacuum test – Optical setup

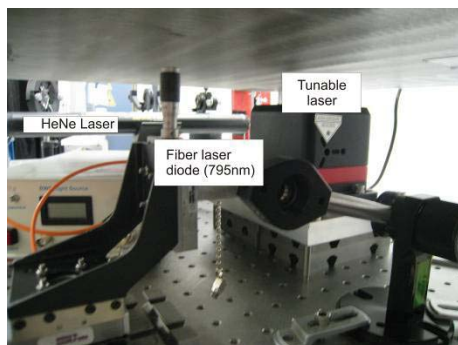
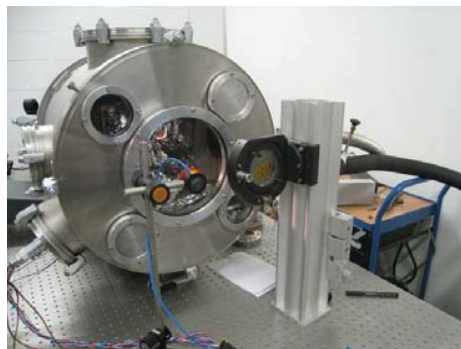
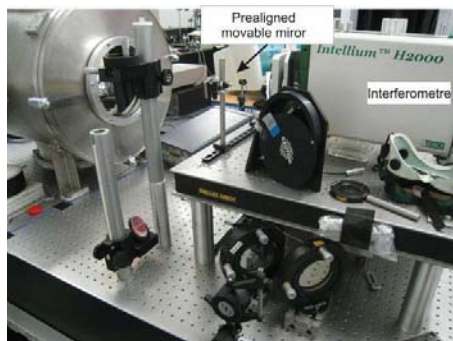


Figure 5: Optical setup and vacuum test chamber

The optical setup is mainly composed of a Fizeau interferometer coaligned with 5 laser lines (from 633 nm to 785 nm). In the WFE configuration for PTR testing a mirror is placed outside the vacuum chamber in order to realise the interferometric cavity. A movable prealigned mirror can be placed in front of the entrance optical window to direct laser beams for the efficiency measurement configuration. A photodetector is placed before the cavity mirror on the exit side.

III. RESULTS

A. PTR & DCG Spectral characterisation

1) Spectral curves:

The curves presented on Figure 6 and Figure 7 have been acquired with the setup presented on Figure 2. These curves correspond to the absolute diffraction efficiency of the specified devices. Fresnel reflections have been extracted out of the measurements. The central curve has been acquired by tilting the grating at the angle which maximises the design wavelength, 656 nm in PTR case and 687 nm for DCG. The others curves have been acquired by changing the incidence angle of light arriving on the grating. This rotation changes the central wavelength of the spectrum by modifying the Bragg condition occurring in the grating. In the case of PTR grating the maximum of efficiency follows the same evolution in function of TE and TM polarisation state, when the evolution of that polarisation state is quite different in the case of DCG grating. Absolute diffraction efficiencies of DCG grating are relatively higher than those measured on PTR grating for the grating analysed. The reason is due to the thickness and the index modulation achievable practically in PTR material compared to DCG grating. Due to technology of PTR grating only thick sensitive material (a few millimetres) is achievable when DCG could be provided with a few μm thick. The thickness is inversely proportional to the bandwidth. So because ESA requirement gives large spectral band, efficiency has to decrease to fit to the bandwidth.

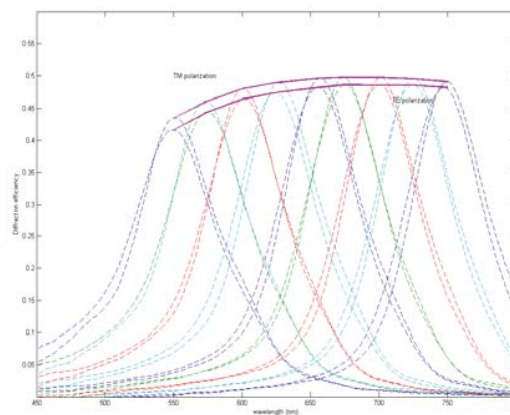


Figure 6: Diffraction efficiency of PTR grating. The upper line corresponds to the TM polarization when the line below is associated to TE polarization.

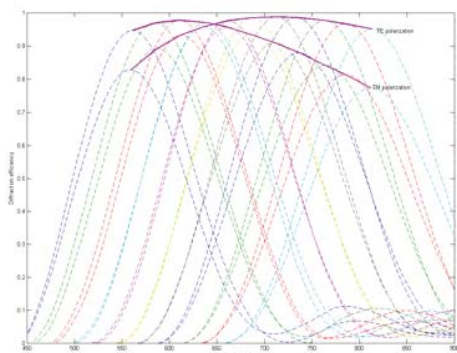


Figure 7: Diffraction efficiency of O2B-DCG grating.

2) Polarization sensitivity:

For Earth Observation polarisation sensitivity is a fundamental parameter [6]. The polarisation sensitivity is calculated from the experimental efficiency maximum at different Bragg conditions. Polarisation sensitivity is defined as

$$S_{pol} = \frac{\eta_{max}^{TE} - \eta_{max}^{TM}}{\eta_{max}^{TE} + \eta_{max}^{TM}} \quad (1)$$

With η_{max}^{TE} and η_{max}^{TM} the maximum of grating efficiency in TE and TM polarization state respectively. The graphs shown in Figure 8 and Figure 9 represents the polarisation sensitivity of PTR and DCG grating respectively.

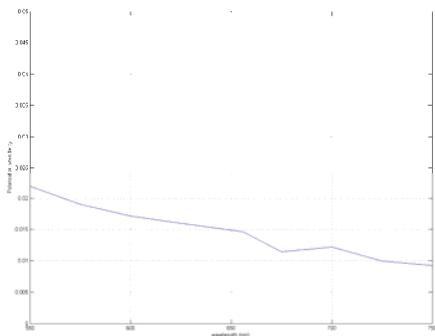


Figure 8: Polarisation sensibility of PTR sample

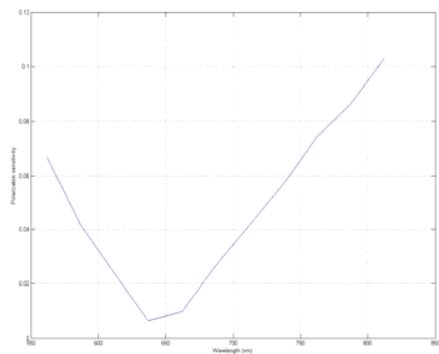


Figure 9: Resulting polarisation sensitivity of DCG grating

3) Diffraction efficiency vs field incidence:

On the point of view of Earth observation, efficiency under field incidence is also an important point to measure. Field incidences correspond to the direction associated to the spatial information of the image in the case of a hyperspectral instrument. These directions are in the perpendicular plane of incidence of the one of dispersion direction. The later corresponds to the spectral information of image. In order to have a large swath, VPH gratings have to keep their efficiency properties with field incidence. We performed measurements from 0 to 30° of incidence which correspond to a half swath-angle. After measurements we note that efficiency properties remain stable with field incidence.

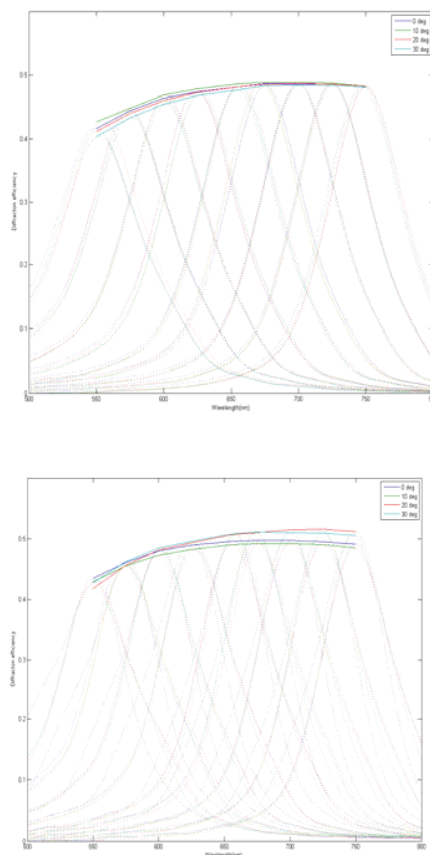


Figure 10: Evolution of the PTR diffraction efficiency with an incidence tilt in the perpendicular plane of light dispersion. 0° to 30° tilt angles are applied.

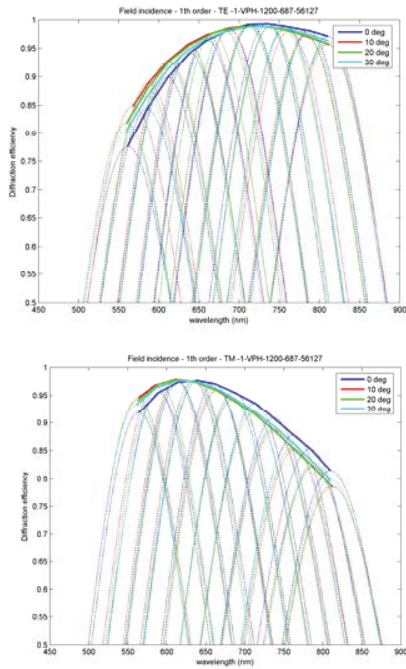


Figure 11: Evolution of the DCG diffraction efficiency with an incidence tilt in the perpendicular plane of light dispersion. 0° to 30° tilt angle is applied.

B. WFE evolution with temperature

PTR and DCG gratings were submitted to thermal vacuum test. During the thermal vacuum test, efficiency and WFE measurements have been performed. The temperature targets are 190K and 310K. Three cycles were realised.

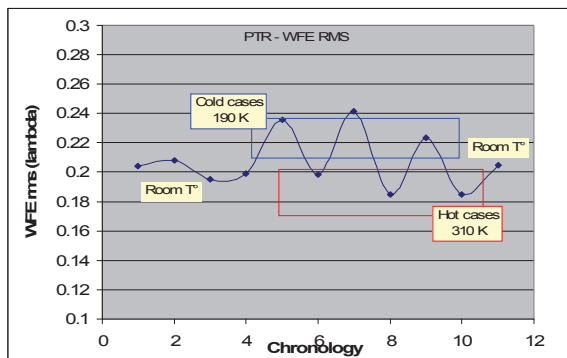


Figure 12: WFE evolution during thermal vacuum test for PTR sample.

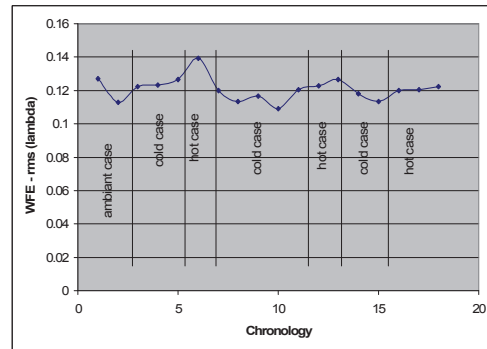


Figure 13: DCG - WFE measurement during thermal test sequence.



Figure 14: DCG - O2B grating - Picture of grating increase of scattering when regulation lamp is switched on.

In the case of PTR, the WFE vary cyclically with temperature. However no permanent degradation was noticed after thermal cycle. The same experiment was made with the DCG gratings. In that case no significant WFE variations were measured. The case O2B grating is presented in Figure 13. One observes that WFE is stable in time and with temperature. The thermal vacuum tests of VBG made with DCG have shown unforeseen property when the regulation lamps have been switched on at low temperature. Both grating (O2B and NIR) became opaque at low temperature (190K) and the scattering of light increased. Figure 14 illustrates this phenomenon which is completely reversible. The sample is recovering its transparency at room temperature. At high temperature this phenomenon did not occur. During apparition of this scattering the properties of the grating WFE and diffraction efficiency were clearly affected. However once the grating becomes transparent again the optical properties recover to normal. The apparition of scattering is attributed to residual water trapped in gelatine resulting from an incomplete drying process by manufacturer. Evaporation when the lamps are switched on followed by a direct condensation could explain this phenomenon.

C. Diffraction efficiency evolution with temperature

PTR and DCG results are presented on Figure 15 and Figure 16 respectively. In both cases no significant variations

are observed. Efficiencies remain stable during time and temperature change. However, in case of DCG grating, efficiency falls down during the increase of scattering due to residual water inside. But grating recovers all its properties at room and high temperature. No permanent degradation is observable.

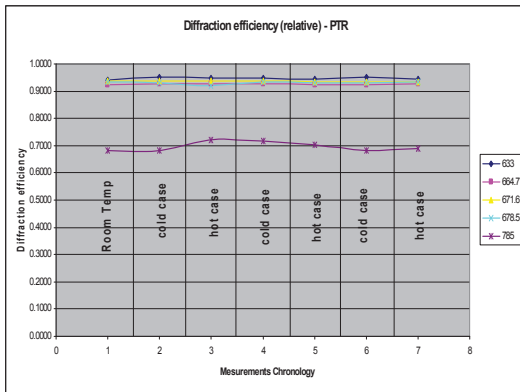


Figure 15: PTR diffraction efficiency vs temperature

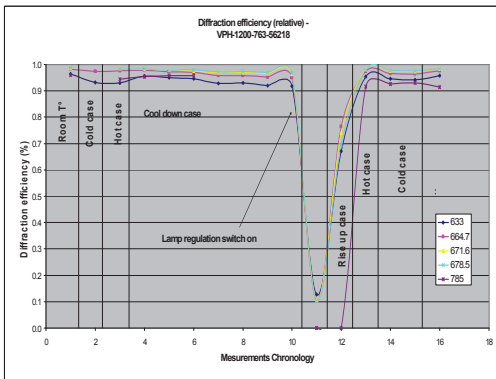


Figure 16: DCG NIR diffraction efficiency evolution with temperature

D. Radiation test

All the samples and gratings have been irradiated with the same doses. Intermediate measurements have been realized.

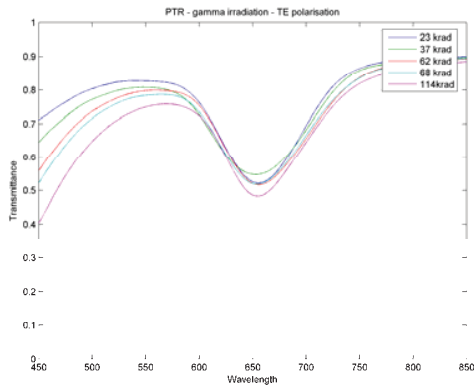


Figure 17: Evolution of the grating transmittance (0th order of diffraction) in function of the level of irradiation. TE polarisation is presented

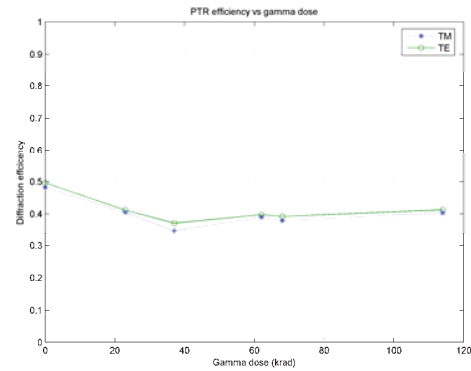


Figure 18: Evolution of the absolute PTR diffraction efficiency in function of the gamma dose received by the grating.

The evolution of PTR diffraction efficiency after receiving increasing gamma dose is presented in Figure 17 and Figure 18. The experiment exhibits an efficiency decreasing with gamma dose. However it seems that the efficiency is stabilising. Same experiment was performed on DCG grating. In that case no significant variation is measured with the gamma dose. The results are shown on Figure 19 to Figure 20. In conclusion DCG grating remains stable with radiation when PTR exhibit efficiency decrease.

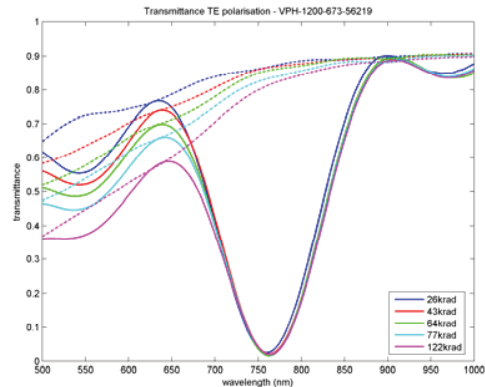


Figure 19: Evolution of the grating transmittance in function of the level of irradiation. TE polarisation (left), TM polarisation (right).

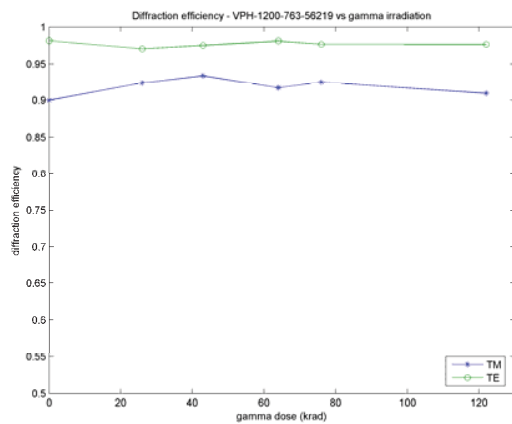


Figure 20: Evolution of the DCG diffraction efficiency in function of the gamma dose received by the grating.

IV. CONCLUSIONS

The objectives of the project were first to evaluate different kinds of VBG technologies and secondly to experimentally compare them. The special properties of VBGs make them interesting for spectrometry applications where high spectral resolution, low level of straylight and low polarisation sensitivity are required. Selected technologies were DiChromated Gelatine (DCG) and PhotoThermal Refractive glass (PTR). The presented paper was dedicated to the experimental evaluation of those selected VBG technologies.

In conclusion, both technologies seem suitable for space applications. However, the bandwidth achievable with DCG grating is larger than those achievable with PTR due to the thickness of the active material. If large bandwidth is required for PTR, the price to pay is a drastic reduction of efficiency on the overall band counter to Dichromated gelatin which could achieve very high efficiency on large bandwidth, close to 100% on both polarisations.

Concerning the environmental experiments, both grating technologies are surviving to vacuum thermal test without any degradation. However, about the radiations, a light modification on efficiency properties is noticed for PTR grating, when DCG does not have any modifications and remains stable.

V. ACKNOWLEDGEMENT

The authors would like to thanks the European Space Agency, which has funded this research under ESA contract N° 22616/09/NL/RA.

The authors would also like to thanks the societies Optigrate and Kaiser Optical System for their support, respectively, on PTR grating and DCG grating.

VI. REFERENCES

[1] H. Kogelnik, "Coupled-wave theory of thick hologram gratings", Bell Syst. Tech. J. 48, 2909–2947 (1969)

[2] M. G. Moharam and T. K. Gaylord, "Rigorous coupled-wave analysis of planar-grating diffraction," J. Opt. Soc. Am. 71, 811-818 (1981)

[3] M. G. Moharam and T. K. Gaylord, "Three-dimensional vector coupled-wave analysis of planar-grating diffraction," J. Opt. Soc. Am. 73, 1105-1112 (1983)

[4] TRAQ - Tropospheric Composition and Air Quality, Candidate Earth Explorer Core Mission, Report for Assessment, ESA SP 1313/6, November (2008)

[5] FLEX – Fluorescence Explorer, Candidate Earth Explorer Core Mission, Report for Assessment, ESA SP 1313/4, November (2008)

[6] R.B. Myneni, J. Ross "Photon-Vegetation Interactions" Springer-Verlag (1991)

[7] GMES Sentinels 4 and 5 – Mission Requirements Document, ESA EOP-SMA/1507/JL-dr, 2 April (2007)

[8] P.-A. Blanche, P. Gailly, S. Habraken, P. Lemaire, and C. Jamar, "Volume phase holographic gratings: large size and high diffraction efficiency," Opt. Eng. 43, 2603–2612 (2004)

[9] P.A. Blanche, S. Habraken, P. Lemaire, C. Jamar, "Diffracted wavefront measurement of a volume phase grating at cryogenic temperature", Applied Optics 45(27), 6910-6913 (2006)

[10] S. C. Barden, J. A. Arns, and W. S. Colburn, "Volume-phase holographic gratings and their potential for astronomical applications," in Optical Astronomical Instrumentation, S.D'Odorico, ed., Proc. SPIE 3355, 866–876 (1998)

[11] J. A. Arns, W. S. Colburn, and S. C. Barden, "Volume phase holographic gratings at ESO," in Current Developments in Optical Design and Optical Engineering VIII, R. E. Fischer and W. J. Smith, eds., Proc. SPIE 3779, 313–323 (1999)

[12] L.B. Glebov, "Volume hologram recording in inorganic glasses", Glass Science and Technology 75 C1, 73-90 (2002)

[13] L.B. Glebov L. Glebova, E. Rotari, A. Gusarov, and F. Berghmans, "Radiation-induced absorption in a photo-thermo-refractive glass", Proc. of SPIE 5897 on Photonics for Space Environments X , paper 5897-0J (2005)

[14] V. Rotar, L. Glebova, A. Gusarov, F. Berghmans, L. Glebov, "Effect of Ionizing Radiation on Volume Diffractive Gratings in PTR Glass", Solid State Diode Laser Technology Review, Technical Digest (2007)

[15] O.M. Efimov, L.B. Glebov, V.I. Smirnov, "High-frequency Bragg gratings in photothermorefractive glass" Optics Letters, 23, 1693-1695 (2000)